Nov 7th, 12:00 AM - Nov 8th, 12:00 AM

Stressed Skin Design of Steel Sheeting Panels – Part 2: Shear Panels with Sheeting Fixed on all 4 Sides

A. M. Wrzesien

James B. P. Lim

I. A. MacLeod

R. M. Lawson

Wei-Wen Yu International Specialty Conference on Cold-Formed Steel Structures
St. Louis, Missouri, U.S.A., November 7 & 8, 2018

Stressed skin design of steel sheeting panels – Part 2: Shear panels with sheeting fixed on all 4 sides

A.M. Wrzesien[1], J.B.P. Lim[2], I.A. MacLeod[3] & R.M. Lawson[4]

Abstract

In this paper, the strength and stiffness of different roof panels were investigated, in order to establish their ability to act as in-plane diaphragms for stressed skin design of cold-formed steel portal frames. A total of 6 roof panels, approximately 3 x 3m, were examined by testing with sheeting profiles fixed on 4 sides. A variety of sheeting profiles in two industry standard thicknesses of 0.5 and 0.7mm were tested, all using top-hat shaped purlins fixed with self-drilling, self-tapping screws. The experimental strength and stiffness of each panel were then compared against existing design methods. The Finite Element Analysis (FEA) modelling techniques were also presented and validated against series of full-scale tests. The FEA results have shown that the 'true' level of loading transferred via shear connector screws was on average 13% lower than that assumed by standard design methods. On the contrary, seam connections failure, according to FEA results, have governed a design in all of the analysed cases and the analytical method overestimated shear resistances of the panels by 45% and 35% in case of 0.5mm and 0.7mm thick sheeting profiles respectively. It was demonstrated that FEA results have represented the upper bound of experimental shear stiffness, with a very close prediction for 0.5mm thick sheeting profiles. Overall all, the tested panels demonstrated an average 41% greater flexibility then this predicted using FEA models.

[1] Lecturer, School of Engineering & Computing, University of the West of Scotland, Paisley, UK
[2] Reader, Department of Civil and Environmental Engineering, The University of Auckland, Auckland, NZ
[3] Emeritus Professor, Department of Civil and Environmental Engineering, The University of Strathclyde, Glasgow, UK
[4] Professor, Department of Civil and Environmental Engineering (C5), University of Surrey, Guildford, UK

Introduction

Stressed skin action takes into account the inherent resistance and stiffness of the metal cladding in a 3D analysis of the whole building. It has been demonstrated through extensive research that stressed skin action can reduce or eliminate the need for wind bracing. It reduces sway deflections under horizontal forces and also reduces the outward movement of the frame under vertical load. Stressed skin design was originally researched and published by Bryan (1973) and design recommendations were first presented in the 'European recommendations for the stressed skin design of steel structures' ECCS - XVII - 77-1E (1977). This document formed the foundation for later publications such as: 'Manual of stressed skin diaphragm design' Davies and Bryan (1982), BS 5950-9 (1994), ECCS TC7 (1995) and subsequently Eurocode 3 BS EN 1993-1-3 (2006).

The basic idea behind the stressed skin design is to recognize the ability of cladding profile to act as the 'web' of a cantilever beam, as shown in Figure 1 Typical cantilever shear panel as illustrated in BS 5950-9 (1994), pp.2

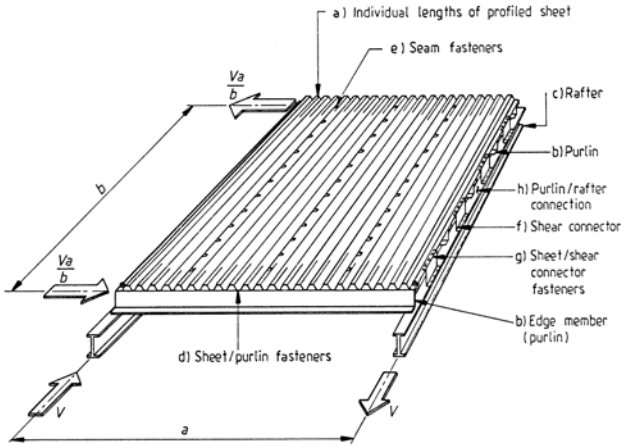

Key
a is the width of the shear panel in a direction perpendicular to the corrugations (in mm);
b is the depth of the shear panel in a direction parallel to the corrugations (in mm);
V is the applied force on the shear diaphragm (in kN).

Figure 1 Typical cantilever shear panel as illustrated in BS 5950-9 (1994), pp.2

A designer can, therefore, choose to model the roofing and cladding panels acting in shear to offer lighter design of the low-rise clad frame. The cladding panels, however, due to their inherent stiffness would carry the same loads regardless of whether they are included in analysis or not. By ignoring the stressed skin action, excess force may be transferred to the roof panel and to the gable frame causing rafter or purlin failure (Wrzesien et al. (2015)).

Roof systems are consistently evolving often leaving existing standards out-of-date. To the author's knowledge, since the last tests on the double skin roof systems by Davies and Lawson (1999) little research had been performed on current roof systems in terms of stressed skin performance. The author's objectives were to conduct an experimental study of different roof panels in order to validate the relevance of the existing state of the art analytical methods for predicting shear resistance and stiffness of modern roof panels.

The novel aspects of this experimental research were as follows:

1) The typical connection detail for purlin to rafter connections, recognised by the BS 5950-9 (1994), includes C or Z purlins connected to the rafters through a web cleat (see Figure 2a). Such a detail has relatively low stiffness in shear unless heavy web cleats are used. However, the use of modern top-hat shaped purlins can simplify the connection detail and improves purlin to rafter connection stiffness (see Figure 2b).

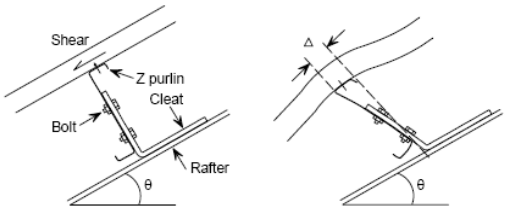

1) Shear deformation of typical Z purlin connection

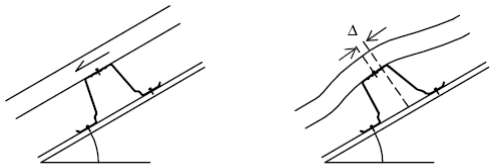

2) Shear deformation of the top-hat purlin connection

Figure 2. Shear deformation of two types of purlin/rafter connection details

2) BS 5950-9 (1994) recommends that the net thickness of the roof or wall sheeting profile should not be less than 0.55mm. Thinner steel, however, is

often used to manufacture cladding profiles and liner trays and the shear performance of very thin panels was investigated. In fact, it is common in the industry that coil of 0.48mm net thickness (excluding coating) is used for manufacturing wall/roof sheeting.

Test set-up for panel assembly

A novel type of purlin connection detail was investigated for a range of cladding types following the recommendations, given in clause 11.4 of BS 5950-9 (1994). Each test was carried out on a cantilever panel of the approximately 3m x 3m subject to shear force, as shown in Figure 3. The test set-up consisted of cold-formed steel double lipped channels of 3mm thickness for the rafters, top-hat shaped purlins of 61mm depth x 1mm thickness and top-hat for the shear connectors, as shown in Figure 3c. The left-hand side rafter was fixed at both ends and the load was only applied through the right-hand side free rafter. The free rafter was placed on a galvanized steel plates lined with PTFE sheets (i.e. Teflon) to minimise the friction between the free rafter and the concrete floor.

Using the test recommendations in BS 5950-9 (1994), each panel was loaded in four stages:

1) Bedding down – the panel was loaded continuously up to approximately 80% of the serviceability loading; this load was maintained for 15 min. and then removed.
2) Acceptance test - the load was reapplied up to approximately 80% of the calculated shear capacity of the panel; this load was maintained for 15 min and released.
3) Strength test – the panel was reloaded until it reached the load equal to the calculated shear capacity of the panel; this load was maintained for 15 min. and released.
4) Failure test – the panel was loaded until failure of the specimen (i.e. until no increase in load was recorded).

At each stage of testing, the displacements and shear force were logged. The panel's displacement was measured by linear displacement transducers and overall deflection (δ) was calculated from the formula:

$$\delta = \delta_1 - \delta_2 - [(a/b)(\delta_3 - \delta_4)] \quad (1)$$

Where:
$\delta_{1...4}$ – defection of the four corners (as shown in Figure 3a)

a – width of the shear panel
b – depth of the shear panel in the direction parallel to the corrugations

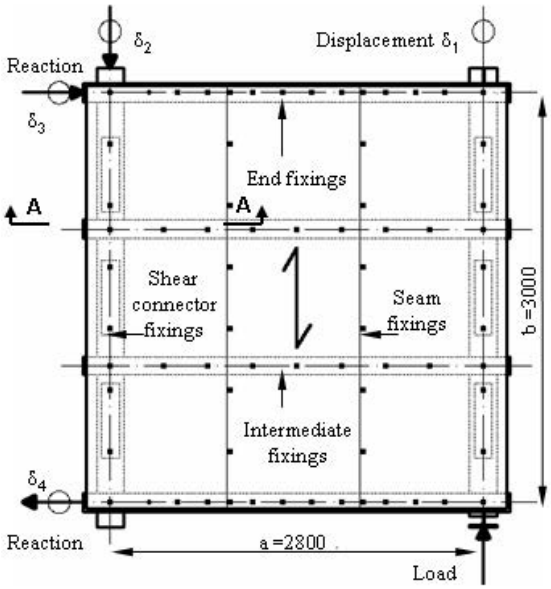

a) Plan view b) Front view – clad roof panel

a) Front view – bare roof panel

Figure 3 Test arrangement of the shear panel test

Rafters and purlins

All the primary and secondary structural members used in the experimental study were manufactured in cold-formed processes from hot-dipped galvanized steel sheets. The back-to-back lipped channel section beam of 400mm depth and 3mm thickness (denoted C40030) was used as a rafter member as presented in Figure 4a. In the case of purlin members, cold-rolled galvanized steel top-hat section (denoted TH) of the geometry shown in Figure 4b, were used (Uzzaman et al. (2016)).

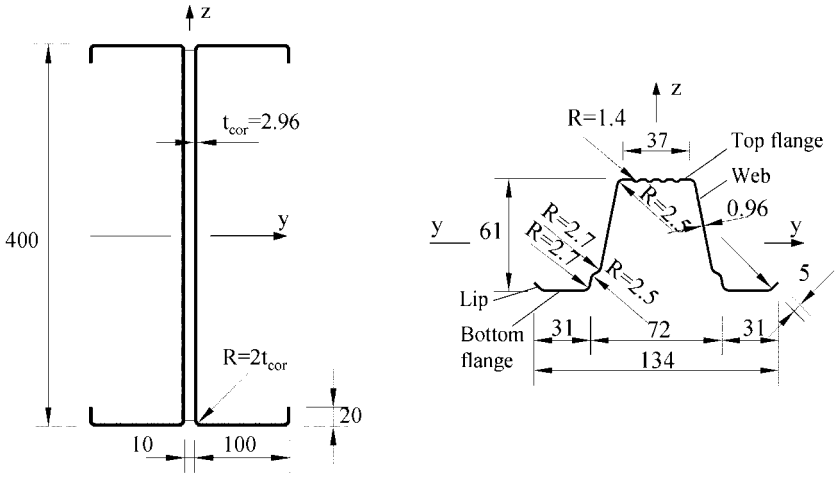

A=36.72cm^2, Iy=8216.46cm^4, Iz=657.48cm^4

A=2.21cm^2, Iy=12.16cm^4, Iz=26.85cm^4

a) Rafter – 2C 40030

b) Top-hat purlin – TH 6110

Figure 4 Dimensions of the component cross-sections (mm)

The mechanical properties of steel pieces, cut out from steel channels and top-hat sections, were established experimentally according to BS EN 10002-1:2001 (2001). Based on test data, average values of the yield strength ($f_{y,a}$) and the ultimate tensile strength ($f_{u,a}$) were established based on three repeated tests and are presented in Table 1. The grade of steel along with the standard which the steel complies to is also listed in that table. Both the nominal thickness (t) and the thickness excluding the coating (t_{cor}) as well as the nominal yield strength ($f_{y,nom}$) and the nominal ultimate strength ($f_{u,nom}$) are listed in Table 1.

Table 1 Steel characteristics of the components

Section name	Steel Grade	t	t_{cor}	$f_{y,nom}$	$f_{u,nom}$	$f_{y,a}$	$f_{u,a}$
		mm	mm	N/mm^2	N/mm^2	N/mm^2	N/mm^2
C 40030	S350GD +Z275[1]	3.0	2.96	350	420	383	483
TH 6110	S550GD +AZ150[1]	1.0	0.96	550	560	580	599

[1] BS EN 10326:2004 (2004)

Sheeting profiles

The test roof panels were chosen to cover a range of sheeting profiles offered by the industry. Two different types of sheeting profiles were considered, shown in Figure 5. Type 1 is the typical trapezoidal sheeting profile and Type 2 is the trapezoidal sheeting with additional stiffeners of 1mm height rolled into every trough. The dimensions of each profile are presented in Table 2. Each sheeting panel was considered in two thicknesses of 0.5 and 0.7mm.

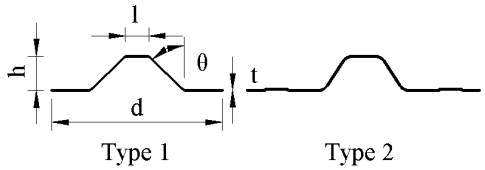

Figure 5 Different sheeting profiles

Generally, two steel sheets of 0.5 and 0.7mm nominal thickness were used to manufacture the investigated sheeting profiles. The 0.5 and 0.7mm thick coil finished with leather-grain embossed PVC (Plastisol) were used for all on the weather sheets. The description of the steel used is presented in Table 3 including the net thickness of the steel core and mechanical properties of the steel based on the average values obtained from Mills Test Certificates. The screw configuration followed the assembly manual provided by sheeting manufacturer (Steadmans (2014)).

Table 2 Sheeting profile dimensions

Profile name	Type (see Figure 5)	Height h (mm)	Thickness t (mm)	Pitch d (mm)	Width l (mm)	Angle θ (°)
AS34	1	34	0.5&0.7	167	23	45
AS30	2	30	0.5&0.7	200	30	33
AS24	2	24	0.5&0.7	167	20	34

Table 3 Steel characteristic for the investigated profiles

Steel coil type	Steel Grade	t	t_{cor}	$f_{y,nom}$	$f_{u,nom}$	f_y	f_u
		mm	mm	N/mm^2	N/mm^2	N/mm^2	N/mm^2
0.5 Plastisol	S250GD +AZ150[1]	0.5	0.48	250	330	334	405
0.7 Plastisol	S250GD +AZ150[1]	0.7	0.65	250	330	301	380

[1]BS EN 10326:2004 (2004)

Analytical predictions of the shear resistance and flexibility of lapped joint

Many semi-empirical formulas for predicting the shear resistance of screw joints have been published, i.e. Baehre and Berggren (1973), ECCS TC7 No. 21 (1990), Peköz (1990), Toma et al. (1993), BS 5950-5 (1998) and BS EN 1993-1-3 (2006). According to the study by Wrzesien et al. (2018) closes correlation with test results was obtained using Toma et al. (1993) design formula for the shear resistance of lapped joints. In case of predicting a flexibility of the lapped joint connection, Wrzesien et al. (2018) had demonstrated that existing formula developed by Zadanfarrokh and Bryan (1992), with a suggested flexibility reduction factor n_{pf}=0.4, can be used with sufficient accuracy. Presented above formulas were therefore used in this paper and shear resistances and flexibility values are presented in Table 4. The maximum experimental values and characteristic experimental values according to Wrzesien et al. (2018) were also included in Table 4 for comparison. A significant scatter of the results can be observed between characteristic values (lower bound) and the maximum value (upper bound) with the analytical value falling in between (also see in Figure 8).

Table 4 Resistances and flexibilities of the individual joints used for shear diaphragm calculations

Test designation	Resistance					Flexibility				
	Source	F_s kN	F_{sc} kN	F_p kN	$F_{pr,s}$ kN	Source	s_s mm/kN	s_{sc} mm/kN	s_p mm/kN	$s_{pr,s}$ mm/kN
T1, 3, 5	Max. exp. Wrzesien et al. (2018)	1.23	*	*	9.07	Max. exp. Wrzesien et al. (2018)	0.25	*	*	0.07
	Characteristic exp. Wrzesien et al. (2018)	0.81	*	*	7.07	Characteristic exp. Wrzesien et al. (2018)	0.41	*	*	0.09
	Toma et al. (1993)	1.08	2.08	1.83	8.32	Zaharia and Dubina (2006)	0.46	0.34	0.37	0.14
T2, 4, 6	Max. exp. Wrzesien et al. (2018)	2.07	*	3.28	9.07	Max. exp. Wrzesien et al. (2018)	0.15	0.31*	0.31	0.07
	Characteristic exp. Wrzesien et al. (2018)	1.30	1.90*	1.90	7.07	Characteristic exp. Wrzesien et al. (2018)	0.29	0.34*	0.34	0.09
	Toma et al. (1993)	1.60	2.13	1.93	7.61	Zaharia and Dubina (2006)	0.34	0.28	0.30	0.14

* component tests on lapped joints were not carried out

An analytical method for predicting the shear behaviour of roof diaphragms

The analytical method presented in the BS 5950-9 (1994) and adopted by BS EN 1993-1-3 (2006) was used to establish the shear resistance and the shear flexibility of the investigated roof diaphragms. The sheeting profiles were fixed on four sides. The set of input values required to evaluate the shear characteristic of each tested diaphragm is presented in Table 5. The shear resistance and flexibilities of individual fasteners, used in calculations, are summarised in Table 4. The resistance and flexibility of tested diaphragms were only evaluated based on the shear resistance and the shear stiffness of lap joints according to Toma et al. (1993) and Zaharia and Dubina (2006). It was done so results of Finite Element Analysis with the same input data can be compared against hand calculation method presented in the design code. The set of input values used for both FEA and hand calculations is presented in Table 4 and denoted as 'Anl.'. The following notations were used in order to identify two most critical modes of failure according to BS EN 1993-1-3 (2006):
V_s – seam capacity,
V_{sc} – shear connector fasteners capacity.
The overall flexibility of the shear panel was denoted as (c). The output of the hand calculations is presented further in Table 6

Finite Element idealisation of the shear panel test

The general purpose finite element program ABAQUS was used for this study. The model was solved statically, with both geometric and material nonlinearities taken into account.

In order to cut computational time, a crude method of modelling behaviour of screw connections was presented using the ABAQUS standard S4R shell element and Cartesian Connector Element. The screws were modelled using the node-based connector with elastic-perfectly plastic load-displacement characteristic. The calculated data according to Toma et al. (1993) and Zaharia and Dubina (2006) and summarised in Table 4 were used as an input. Parameters such as: thickness of the connected parts, grade of steel, screw diameter, size and type of the washer, are expected to contribute to the performance of screw joints. For this reason, the FEA idealisation was validated against experimental data published by Wrzesien et al. (2018).

Table 5 Input parameters used in analytical method

Test designation	t_{cor}	n_s	n_{sc}	n_p	n_{sh}	n_f	p_{end}	p_{int}	u	I_y	K
							mm	mm	mm	mm^4	
T1 AS34/0.5	0.48	8	6	4	3	6	167	334	194	15959	0.070
T2 AS34/0.7	0.65	8	6	4	3	6	167	334	194	21574	0.070
T3 AS30/0.5	0.48	8	6	4	3	5	200	400	230	14253	0.054
T4 AS30/0.7	0.65	8	6	4	3	5	200	400	230	19285	0.054
T5 AS24/0.5	0.48	8	6	4	3	6	167	334	193	6854	0.047
T6&7 AS24/0.7	0.65	8	6	4	3	6	167	334	193	9271	0.047

t_{cor} – sheet thickness excluding coating

n_s – number of seam fasteners excluding those passing through sheet and purlin

n_{sc} – number of shear connectors fasteners along the one side of the sheet

n_p – number of purlins within the diaphragm

n_{sh} – number of sheets within the diaphragm

n_f – number of fasteners per sheet width at the end of the sheet

p_{end} – fasteners spacing at the end purlin

p_{int} – fasteners spacing at the intermediated purlins

u – perimeter length of a complete single corrugation

I_y – second moment of area of single corrugation about its neutral axis

K – sheeting constant: T1 to T6 according to Table 12, BS 5950-9 (1994), T7 to T8 according to Davies (1986)

According to Wrzesien et al. (2015), in many design cases, it is safer to overpredict the shear stiffness of the roof panel assembly in order to prevent cladding or gable frame failures. For this reason, joint stiffness values presented in Table 4 were multiplied by the factor of 10 to match the upper bound experimental stiffness. The comparison of the test results against crude FEA idealisations for the seam connection between two 0.5mm thick sheeting profiles

and 3mm thick channel section to 1mm thick top-hat sections are shown in Figure 8.

A contact interaction with hard normal behaviour and frictionless tangential behaviour was modelled between all surfaces (steel plates). Both geometric and material nonlinearities were taken into account. The elastic-perfectly plastic model was used for all of the steel plates based on the Young's Modulus E=210GPa, Poisson's ratio of 0.3 and relevant yield strengths (f_y) according to Table 1 and Table 3.

Due to the complexity of the FEA model relatively coarse mesh of 10mm was used for all of the components. It should be noted that the same mesh size was used to model component tests on lap joints and a satisfactory representation of the true behaviour was obtained hence the same mesh size was used for full-scale models. The mesh size sensitivity study was not carried out.

The boundary conditions for the FEA model are presented in Figure 6. The left-hand side fixed rafter was restrained against translations UX=UY=UZ=0 at both ends. Both fixed and free rafters (right-hand side) were restrained against vertical translation (UY=0) at the contact surface with the strong floor in order to simulate test support conditions. The load was applied via the web edge of the free rafter as an imposed displacement.

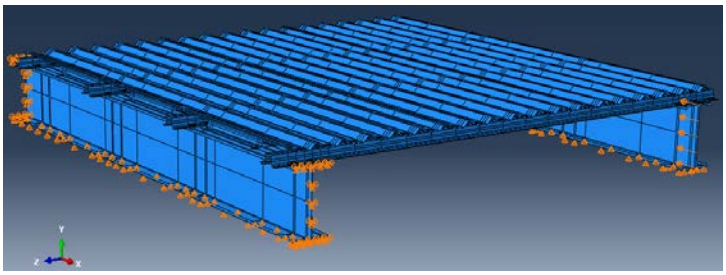

Figure 6 Boundary conditions

Comparison of test results versus Finite Element Analysis

In this section, the results of seven shear roof panels tested with shear connectors are presented. In last test (T7), the shear panel identical to this in test T6 was tested again, so the scatter of the experimental results for both resistance

and flexibility can be established. As presented in Table 6, a 7% difference was recorded between both experimental shear resistance and flexibility of two identical panels.

It should be noted that three distinctive failure modes were observed and these were also captured by the FEA models as shown in Figure 7. In general, all the tests followed similar failure mechanism. First, the sheeting profile distortion was observed followed by holes elongations around seam screws often resulting in pull-out of these screws. At this stage, little shear resistance increase was recorded and loading was continued until local buckling of the top-hat had occurred. The shear connectors failure was not evident in tests T1 to T7 although the analytical method selected this mode as most critical (see Table 6).

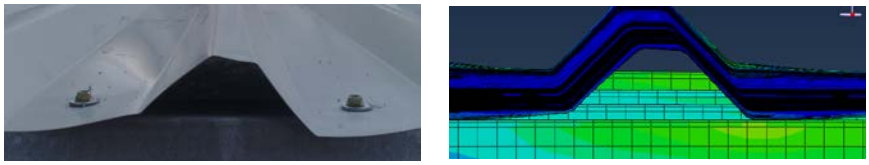

a) Mode 1 - sheeting profile distortion

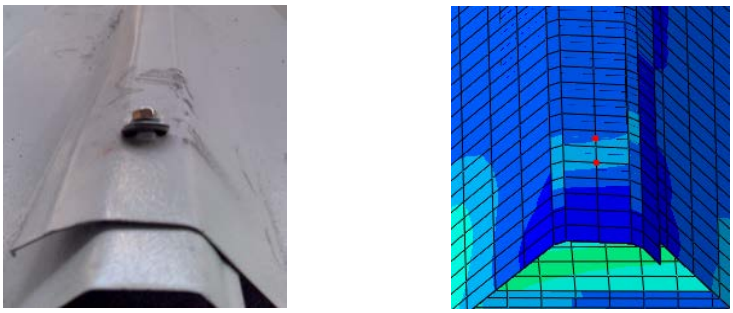

b) Mode 2 - holes elongation around seam screws (loss of watertightness)

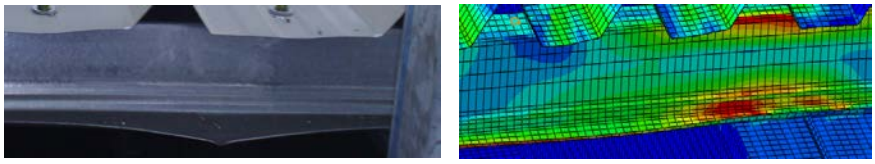

c) Mode 3 - local buckling of the end the top-hat purlin

Figure 7 Failure modes (tests versus FEA)

The load-deflection curves for six tests to failure are presented in Appendix. – Full-scale Results. Photographs of the failure modes observed within each test are also provided in these figures. A peak shear loads (V_T) and respective shear flexibilities (c_T) were calculated from load-deflection curves for each tested panel and are presented in Table 6. The analytical shear resistances (V*) and flexibilities of panels (c) denoted as "Anl." (see Table 6) were calculated, as described in section 'Analytical method for predicting the shear behaviour of roof diaphragms'. In order to identify the value of the shear load triggering the failure of the seam (V_s) and shear connector screws (V_{sc}), shear forces in each Connector element were extracted from FEA results.

It should be noted, that in the case of test T3, the initial test results were not recorded due to equipment malfunction (see Figure 10). The linear load-deflection relationship was used to replace the missing data. Generally in all the tests, tearing of the sheeting around the seam screws (see Figure 7b) contributed largely to the failure of the panels. However, in the case of the diaphragms with 0.5mm thick sheeting, profile distortion (Figure 7a) was also observed in the early stage of loading. Extensive local shear distortion of the profile in test T4 was observed in the early stage of loading, causing higher flexibility than predicted analytically. It is suspected that this unusual behaviour is a result of screw pull-out failure, which due to a large number of fasteners, could not be clearly identified.

Table 6 Shear resistances and flexibilities predictions

Test designation	Model	V_s	V_{sc}	V*	c	V_T	c_T
		kN	kN	kN	mm/kN	kN	mm/kN
T1 AS34/0.5	Anl.	14.88	12.48	12.48	0.55		
	FEA	10.08	14.80	10.08	0.27	19.20	0.27
T2 AS34/0.7	Anl.	19.38	12.78	12.78	0.36		
	FEA	14.14	14.61	14.14	0.21	33.20	0.29
T3 AS30/0.5	Anl.	13.95	12.48	12.48	0.61		
	FEA	10.34	14.19	10.34	0.28	18.20*	0.39
T4 AS30/0.7	Anl.	18.40	12.78	12.78	0.39		
	FEA	14.25	14.44	14.25	0.18	34.50	0.63*
T5 AS24/0.5	Anl.	14.88	12.48	12.48	0.47		
	FEA	9.83	14.54	9.83	0.21	21.90	0.34
T6 AS24/0.7/1	Anl.	19.38	12.78	12.73	0.33		
	FEA	14.03	14.92	14.03	0.15	34.30	0.30
T7 AS24/0.7/2						36.85	0.28

* Experimental data affected by unexpected behaviour or malfunction of the equipment

Conclusions

A successful application of FEA modelling techniques was demonstrated in predicting the shear behaviour of sheeting panels. When the shear resistances of individual fasteners were established by analytical equation after Toma et al. (1993) (model "Anl."), FEA-predicted peak loads where either close to the experimental results (see Figure 9a, Figure 10a, Figure 11a), or significantly lower than experimental results (see Figure 9b, Figure 10b, Figure 11b). It is expected that the safety margin in FEA predations for 0.7mm thick sheeting profiles could be reduced if experimental values of fastener shear resistance (see Figure 8) were used in the FEA model. The main purpose of work presented in this paper was a comparison of the FEA results versus well established analytical method. Following conclusions can be drawn:

- In all of the analysed cases, the analytical method predicted shear connector screws failure as a critical design criterion. This, however, was not confirmed by either observation during experiments, nor FEA results. The FEA-predicted shear resistance due to the shear connector failure was on average 13% higher than the calculated one. This can be explained by the fact that analytical method ignores the ability to carry direct shear by purlin-to-rafter connection and top-hat ability to carry shear directly to the rafter was confirmed by FEA results.
- The FEA results have demonstrated that the analytically predicted shear resistances of the panels due to the failure of the seam screws are overestimated by the average of 45% and 35% for 0.5mm and 0.7mm thick sheeting profiles respectively. According to FEA results seam connections, failure governs design in all of the analysed cases.
- The FEA analysis suggests that more seam screws should be specified by the manufacturer in order to improve the shear resistance of both 0.5mm and 0.7mm sheeting panels.

In terms of shear flexibilities of the tested panels, the analytical methods offered predictions which were over two times greater than shear flexibilities established using FEA analysis. It should be noted that in the stressed skin design of portal frames, underestimation of the stiffness of the panel, will lead to underestimation of the loads transferred to rigid gables. Test load-displacement curves (see Figure 9, Figure 10, Figure 11) show that FEA results are representing upper bound of shear stiffness, with a very close prediction for 0.5mm thick sheeting profiles. Overall all, the tested panels demonstrated an average 41% greater flexibility then this predicted using FEA models. The FEA modelling techniques presented in this paper are shown to be a more accurate alternative to the well-established analytical method.

Appendix. – Component Result

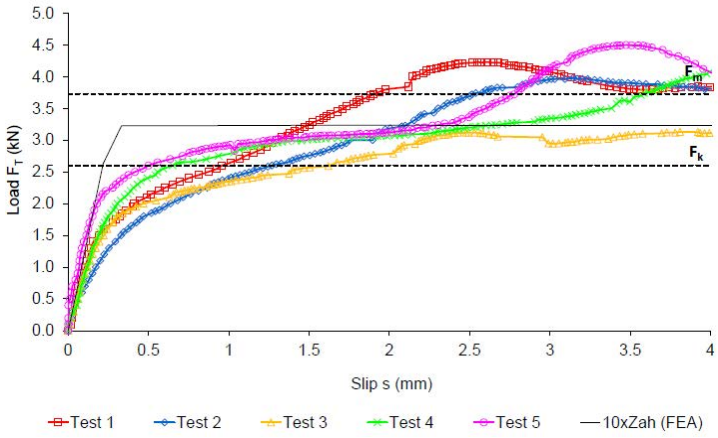

a) 0.7mm to 0.7mm thick steel plates and two screws

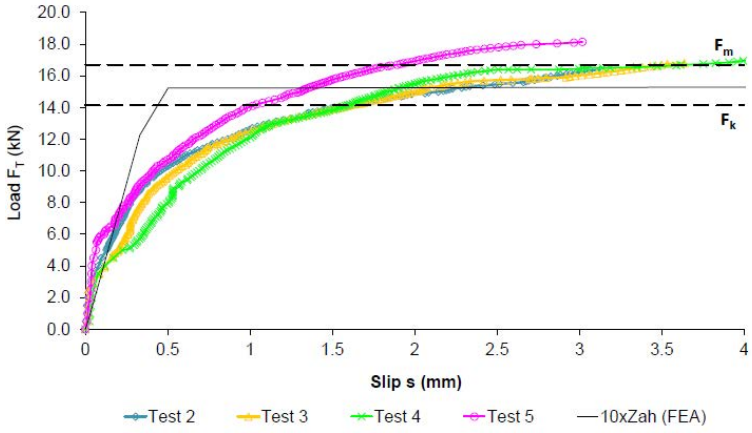

b) 1.0mm and 3.0mm thick steel plates and two screws

Figure 8 Calibration of FEA idealisation versus tests results

Appendix. – Full-scale Results

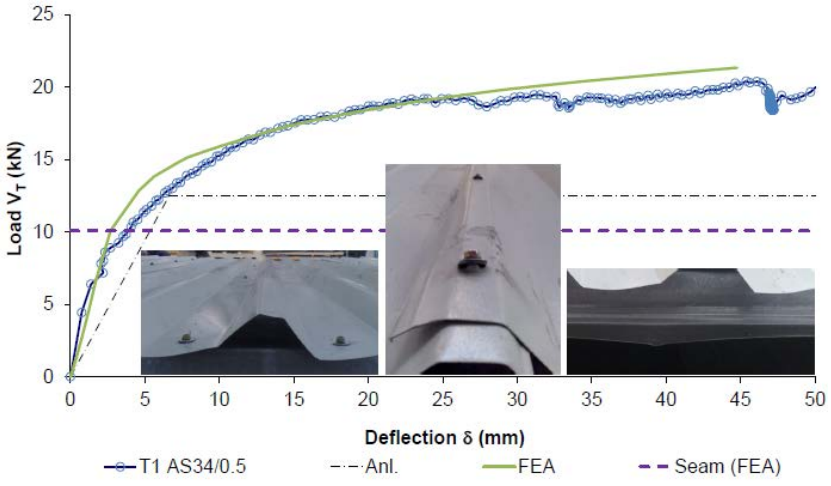

a) Test 1

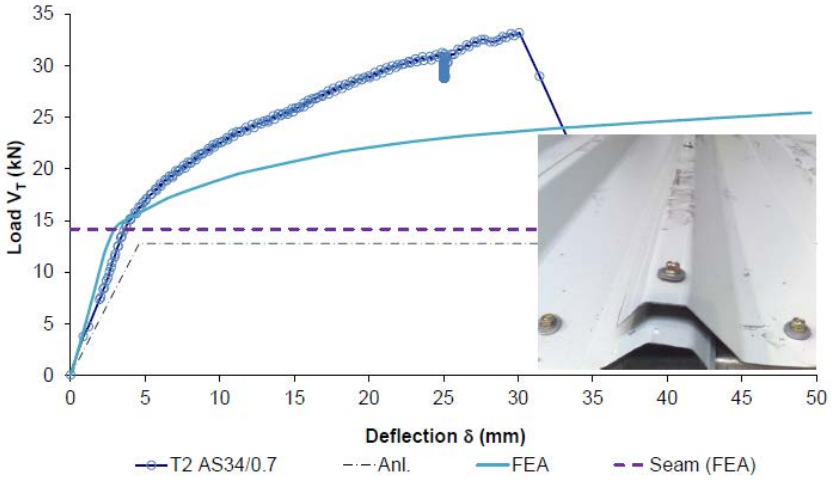

b) Test 2

Figure 9 Load –deflection curves for AS34 sheeting profile

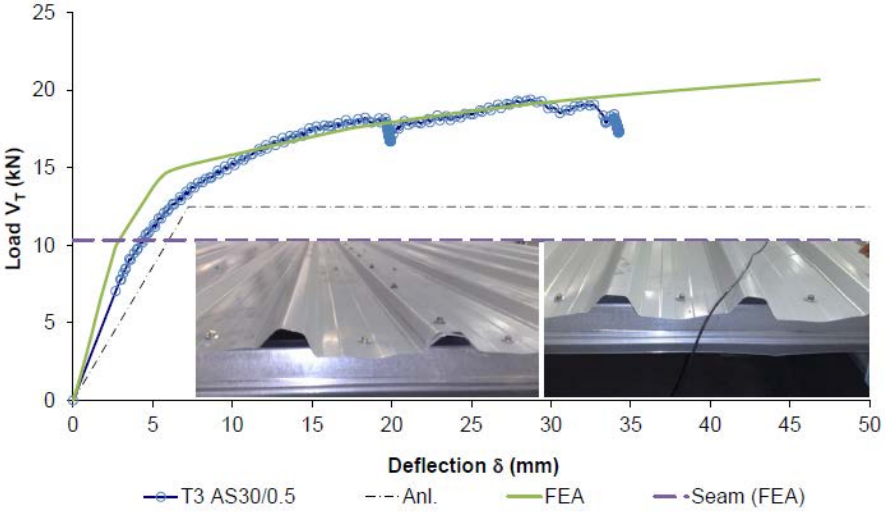

a) Test 3

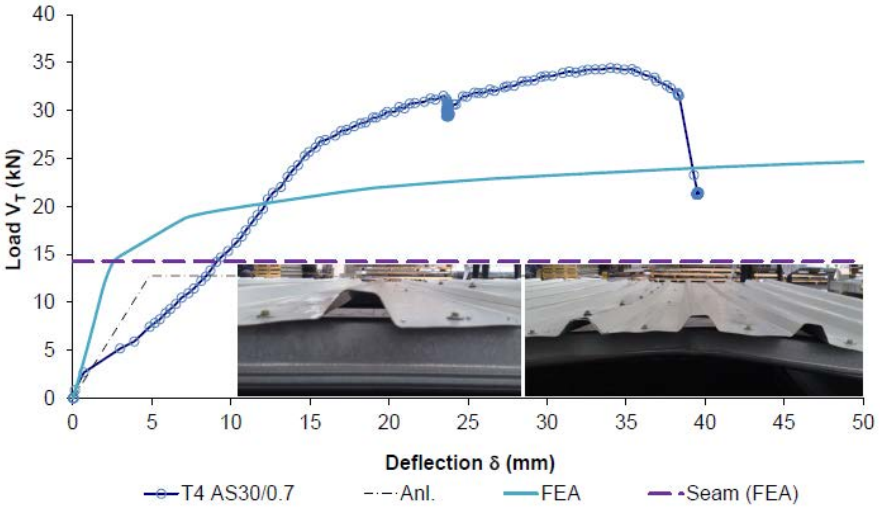

b) Test 4

Figure 10 Load –deflection curves for AS30 sheeting profile

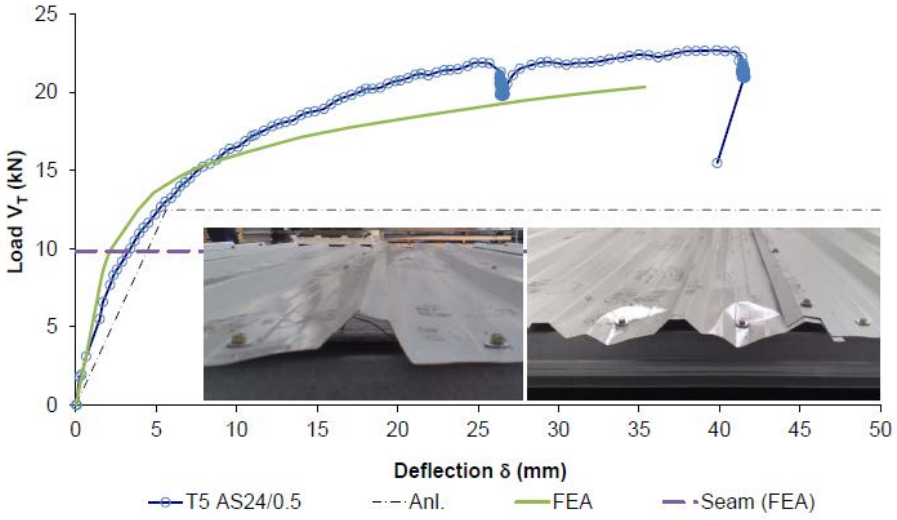

a) Test 5

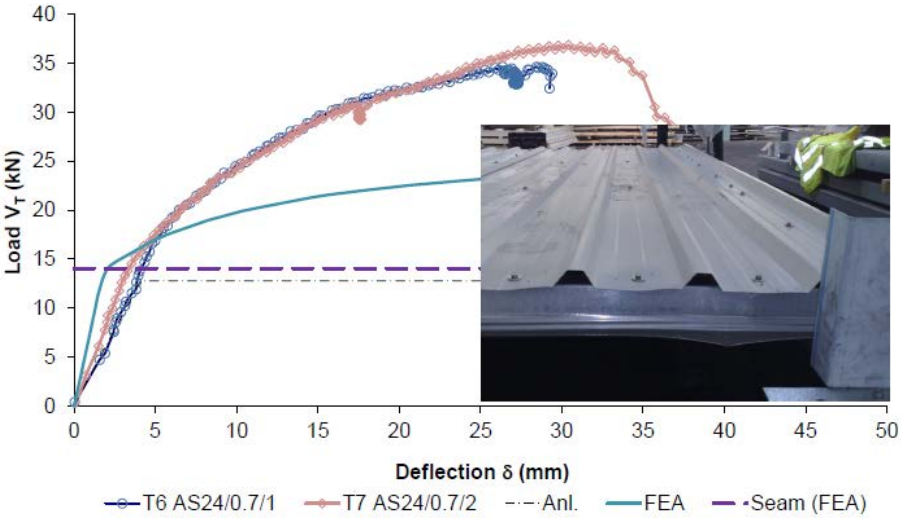

b) Test 6 & 7

Figure 11 Load –deflection curves for AS24 sheeting profile

Appendix. – References

BAEHRE, R. & BERGGREN, L. 1973. Joints in sheet metal panels. Stockholm: National Swedish Building Research.

BRYAN, E. R. 1973. *The stressed skin design of steel buildings, Constrado monographs,* London, Crosby Lockwood Staples.

BS 5950-5 1998. Structural use of steelwork in building *Part 5: Code of practice for design of cold formed thin gauge sections.* London: British Standards Institution.

BS 5950-9 1994. Structural use of steelwork in building. *Part 9: Code of practice for stressed skin design.* London: British Standards Institution.

BS EN 1993-1-3 2006. Eurocode 3 - Design of steel structures. *Part 1-3: General rules - Supplementary rules for cold-formed members and sheeting.* Brussels: European Committee for Standardization.

BS EN 10002-1:2001 2001. Metallic materials - Tensile testing. *Part 1: Method of test at ambient temperature.* Brussels: European Committee for Standardization.

BS EN 10326:2004 2004. Continuously hot-dip coated strip and sheet of structural steels - Technical delivery conditions. Brussels: European Committee for Standardization.

DAVIES, J. M. 1986. A general solution for the shear flexibility of profiled sheets. II: Applications of the method. *Thin-Walled Structures,* 4**,** 151–161.

DAVIES, J. M. & BRYAN, E. R. 1982. *Manual of stressed skin diaphragm design,* London, Granada.

DAVIES, J. M. & LAWSON, R. M. 1999. Stressed skin action of modern steel roof systems. *The Structural Engineer,* 77**,** 30-35.

ECCS - XVII -77-1E 1977. *European recommendations for the stressed skin design of steel structures*, European Convention for Constructional Steelwork, ECCS - XVII -77-1E.

ECCS TC7 1995. *European recommendations for the application of metal sheeting acting as a diaphragm - stressed skin design*, European Convention for Constructional Steelwork, ECCS No. 40.

ECCS TC7 NO. 21 1990. *The design and testing of connections in steel sheeting and sections*, European Convention for Constructional Steelwork.

PEKÖZ, T. 1990. Design of screw connections. *Proceedings of the 10th International Specialty Conference in Cold-Formed Steel Structures.* St Louis, Missouri, USA.

STEADMANS. 2014. Single skin systems [online]. Available: http://www.steadmans.co.uk/wp-content/uploads/2013/03/SingleSkin.pdf [Accessed 20 October 2016].

TOMA, A., SEDLACEK, G. & WEYNAND, K. 1993. Connections in cold-formed steel. *Thin-Walled Structures,* 16**,** 219-237.

UZZAMAN, A., WRZESIEN, A. M., LIM, J. B. P., HAMILTON, R. & NASH, D. 2016. Design of Top-hat Purlins for Cold-formed Steel Portal Frames. *Structures,* 7**,** 113-125.

WRZESIEN, A. M., LIM, J. B. P., MACLEOD, I. & LAWSON, R. M. 2018. Stressed skin design of steel sheeting panels – Part 1: Shear resistance and flexibility of screw lapped joints *Wei-Wen Yu International Specialty Conference on Cold-Formed Steel Structures 2018.* St Louis, Missouri, USA.

WRZESIEN, A. M., LIM, J. B. P., XU, Y., MACLEOD, I. A. & LAWSON, R. M. 2015. Effect of stressed skin action on the behaviour of cold-formed steel portal frames. *Engineering Structures,* 105**,** 123-136.

ZADANFARROKH, F. & BRYAN, E. R. Testing and design of bolted connections in cold-formed steel sections. 11th International Specialty Conference on Cold-Formed Steel Structures, 1992 St. Louis, Missouri, USA. 625-662.

ZAHARIA, R. & DUBINA, D. 2006. Stiffness of joints in bolted connected cold-formed steel trusses. *Journal of Constructional Steel Research.,* 62**,** 240-249.